Stability analyis of robot grasps*

Mark Wright Robert B. Fisher
Department of Artificial Intelligence, Edinburgh University
5 Forrest Hill, Edinburgh EH1 2QL

October 1995

*This work was funded by UK EPSRC Grant GR/J44018.

1 Introduction

The main objective of this feasibility study was to examine the use of range data in grasp synthesis for previously unmodelled objects. In order to do this, a framework previously outlined by Pollard [6] has been modified and extended in simple ways. This report demonstrates that force closed grasps can be synthesised for a number of previously unmodelled objects using range data.

2 Theoretical context

We now provide an outline of the theoretical context in which this work was carried out. This is not intended as a literature review of the large field of robot grasping but a brief statement about our approach and its relevance to other work.

Salisbury [3] built a hand with three fingers, each finger consisting of three independent joints. The hand is capable of force, position or stiffness control. In any given configuration, the hand is capable of exerting a variety of forces through the fingertips. He outlined different contact types, such as frictionless contacts, point contacts with friction and soft fingers, in terms of the degrees of freedom allowed by each contact. He discussed the selection of *internal forces* in an equilibrium grasp. Internal forces are the grasp forces that lie in the null space of the desired wrench; *i.e.* they can be selected according to task requirements and the grasp will still be in equilibrium. A dextrous hand, such as the Salisbury hand, has enough degrees of freedom to be able to select the desired internal forces.

Using Salisbury's contact types, Nguyen [5] synthesized force closure grasps for polyhedral objects. A *force closure* grasp is one that is capable of resisting arbitrary external wrenches (assuming that the grasp forces can be of an arbitrary magnitude). Nguyen synthesizes grasps that maximise the leeway in individual fingertip placement; this means that the grasps are robust with respect to errors in positioning and object modelling error. He observes that for force closure in 3D, the grasp requires either two soft finger contacts or three point contacts with friction or seven frictionless contacts. The grasp synthesis algorithms are presented as geometric constructions. A problem with this work is that it is restricted to polyhedral objects, with no clear extension to arbitrarily shaped objects. Nguyen [4] shows that any force closure grasp can be made stable, by suitable stiffness control of the hand.

Blake introduced perhaps the most elegant theory for grasping of arbitrary shaped objects in 2D [2] and 3D [9]. Blake's criterion for grasp synthesis is to minimise friction. Blake's work makes two main contributions to grasping theory. Firstly, he characterises the profound link that there exists between grasping and visual symmetry. Secondly, in providing a qualitative analysis in terms of extrema of a friction function, he does away with the need for a known coefficient of friction; providing instead *pessimal* and *optimal* grasps with respect the amount of friction required. Blake's analysis is for two fingers and his test of force closure is descended from the simple geometric constructions of Nguyen. The main problem of the approach is there does not appear to be an obvious extension to grasp synthesis involving three, four and more fingers.

Pollard [6] used a wrench space approach to grasp synthesis. She defines a task wrench space which, in its most general form, is the set of all wrenches that can be applied to the object boundary. She then finds a grasp which will span this task wrench space as "efficiently" as possible and which has force closure. The grasp quality criterion used is the radius of the largest sphere, centered at the wrench space origin, which lies inside the convex hull of a chosen grasp's wrench space. See below for more details.

Pollard assumes frictionless contacts and therefore, in the 3D case, at least seven contacts are required. It is therefore aimed at *power grasps*, which use the palm and whole length of each finger to grasp the object, and excludes *precision grasps*, which use only the finger tips. This is a drawback because precision grasps are used much more than power grasps when picking up objects (because power grasps have to "wrap" around the object, which is often prevented by the ground plane), and precision grasps also allow for dextrous manipulation of objects between the fingers. However, as we show, Pollard's approach can easily be extended to include friction, which

means that the number of contacts can be reduced and precision grasps can be planned. This is a good approach to follow for two reasons: unlike Blake's work, it is readily extendable to arbitrary numbers of fingers and unlike Nguyen's work, it is readily extensible to arbitrarily-shaped objects. We have therefore concentrated on this approach in our work.

Little work has examined what type of image data and object models should be used to plan grasps. Blake's work used a contour tracker to describe the object, but both Pollard and Nguyen assumed that geometric models of the object were given. Stansfield [7] used dense range data to build a simple model for grasp planning, composed of surfaces and contours. Grasps were then planned using a rule-based preshaping system [8]. Bard *et al* [1] use dense range data to build models composed of *elliptical cylinders*. These models are more suited to the planning of power grasps, rather than precision grasps, because for many objects, they only provide approximate surface models. Dense range data, such as that provided by a laser striper, is a natural choice for planning grasps, because it allows accurate calculation of surface position and normal, and it is these that determine the wrench space characteristics of the grasp.

With multiple contacts, planning grasps is very complex. With three fingers constrained to lie on a surface, we have a 6 dimensional space of possible digit positions. Pollard [6] uses *grasp prototypes* to constrain the search to a particular portion of the space, and a parallel search method to conduct a brute force search within this portion. A grasp prototype is a stable grasp on some generic object; for an unknown object, a stable grasp can be derived from the nearest grasp prototype. A grasp prototype for a cylinder was used to plan a variety of power grasps, but the big question of selecting which prototype to apply for a given object was not addressed. This approach is similar to preshaping, which is commonly used to cut down the search space for a particular hand configuration (*e.g.* Stansfield [8], Bard [1]).

In order to avoid performing a large search of the range of possible finger positions, we elect to characterise each potential grasp with respect to a specific task requirement — that the internal forces pass through the centre of mass. This decouples the choice of internal force direction for each finger and enables us to produce a qualitative map of the contact quality over the object surface (see below). Other criteria, such as choosing the internal forces so as to minimise the friction, depend on all of contact forces together, so that it is not possible to produce such a map.

3 Pollard's framework

We now give a more detailed description of Pollard's framework. Pollard used the concept of wrench space to define a grasp quality measure of how well a grasp spans the wrenches that are to applied to an object in a given task.

A wrench ω_i can be defined as the set of forces f_i and torques τ_i at contact i combined into a single vector:

$$\omega_i = \begin{bmatrix} f_i \\ \tau_i \end{bmatrix}$$

For a planar problem wrench space is three dimensional. Forces can be applied in the x and y directions and a torque can be applied about the z axis which is perpendicular to the plane. Torques are measured with respect to the center of gravity.

Pollard defines three types of wrench space entity:

- The *limit wrench space* is that portion of wrench space bounded by the convex hull of the wrenches (due to unit force) *that meet the general force and torque constraints of the problem*: $|f_i| = 1$ and $|\tau_i| \leq 1$. This can be visualised as a unit cylinder centered at the origin of wrench space.
- The *object wrench space* is that portion of wrench space bounded by the convex hull of the wrenches, due to unit force, that meet the general force and torque constraints of the problem *and which can be applied to the target object.* The size and shape of the object wrench space is limited by the object geometry, *e.g.* a torque cannot be applied through point frictionless contacts to a circular disc. This can be visualised, for the case of a smooth object boundary, as a continuous line drawn on the surface of the unit cylinder described above. No friction is modelled.
- The *grasp wrench space* is that portion of wrench space bounded by the convex hull of the wrenches that meet the general force and torque constraints of the problem *and form a given grasp on the target object.* The size and shape of the grasp wrench space is limited by the placement of contacts on the target object boundary. This can be visualised as a set of points chosen from the object wrench space line.

The most fundamental test that Pollard applied is whether the grasp is force closed. This is determined by a simple geometric condition, *i.e.* that the convex hull of the grasp wrench space encloses the origin of wrench space. An attractive aspect of Pollard's work is that not just force closure is tested but also how "well" wrench space is spanned. It is possible that a grasp is force closed but that to offset certain task wrenches a huge force will have to be applied at a finger contact. A good grasp is one where only modest forces need to be applied at the fingers to offset any wrench. The grasp quality measure that Pollard used was the radius of the largest sphere with a center at the wrench space origin that fitted within the grasp wrench space (we give examples in the next section).

4 Limitations of Pollard's approach

Although Pollard's approach has much to commend it, there are some limitations which mean it is, as it stands, unsuitable for synthesizing precision grasps for typical multi-fingered hands.

Pollard suggests that the extrema of the object wrench space curve are good candidates for contact placements. She argues that such placements will maximise the grasp quality measure, i.e the radius of the wrench space ball. Although this is true for the examples used by Pollard the following points must be considered:

Force closure requires that the grasp wrench space must *span* wrench space *i.e.* by definition they should be able to offset any wrench applied to the object; a geometric interpretation of this

fact is that the convex hull of the grasp wrench space *encloses the wrench space origin*. Only if the wrench space origin is enclosed can the wrench space ball have a positive radius. This means that an n dimensional wrench space requires that there must be at least $n+1$ linearly independent frictionless point contacts. For the planar case wrench space is three dimensional and therefore four frictionless point contacts are required for force closure. Clearly if there were only 3 contacts then the grasp wrench space could at best only form a plane which could never *enclose* the wrench space origin.

If there are four or more linearly independant contacts in 2D then the grasp wrench space will enclose a volume in wrench space. However, this does not guarantee that the origin of wrench space will be enclosed. The object wrench space extrema chosen must be well spaced out around the limit wrench space cylinder and be of mixed types (maxima and minima).

The examples illustrated by Pollard for the planar case, where wrench space is three dimensional, typically had five contacts which is one in excess of the minimum required for force closure. Under these conditions enclosure of the origin and thus force closure is a likely although not a guaranteed occurrence.

However, if we consider the general three dimensional case then wrench space is six dimensional (three force directions and three torques about these axes). In this case we require at least 7 frictionless point contacts for force closure. Pollard's examples use at least 7 contacts, so there is a high chance that force closure is achieved and that many, if not a majority, of torque extrema are occupied and therefore good force closure assured.

The requirement of 7 contacts means that only power grasps can be planned. If we wish to plan precision grasps and these fingertips are modelled as frictionless contacts then they can never define a hyper-volume in the six dimensional wrench space. In the three dimensional case force closure can only be achieved by a hand with less than seven contacts if friction is considered. Any grasp with low friction can be considered as always "near" singular *i.e.* a thin volume in wrench space.

5 Modifications to Pollard's approach

To overcome the limitations just outlined we suggest two modifications to the basic scheme:

1. Add friction to the analysis thus allowing force closure for smaller numbers of contacts.
2. Choose torque zero crossings (w.r.t the center of gravity) rather than torque extrema as contact points.

Choosing torque zero crossings is a good heuristic for 3 reasons:

- In this project, our task is to pick the object up and perhaps tilt the object in order to fulfil some simple task specification. In this case the task wrench on the object will be due to the gravity vector alone. Because we take the moments with respect to the center of mass, the gravity vector will always lie in the zero torque hyperplane of wrench space. This can be visualised for the planar case as the horizontal plane passing through the origin of wrench space, *i.e.* lying in the force plane. To span the wrenches in this hyperplane a reasonable, though not necessarily optimal, strategy is to choose contact points which lie in this plane in wrench space; these points are the torque zero crossings of the object wrench space and are where the *surface normals of the object pass through the center of mass.*
- We are interested in using precision grasps with perhaps 2-4 fingers and certainly less than the theoretical minimum of 7 for frictionless contacts. Only friction ensures that the grasp wrench space convex hull encloses a hypervolume in wrench space. When friction is small we can envisage this hull as a thin small finite volume. A reasonable strategy to enclose the wrench space origin with such a lamina is to choose torque zero crossings thus placing the lamina in the zero torque hyperplane.

- Finally, such a heuristic provides us with a mechanism for adding further fingers, should they be available. We can add them at other free torque zero crossings thus providing additional coverage of the force plane. Alternatively, we can split a virtual finger already at a torque zero crossing into two new fingers. These fingers can then proceed in opposite directions until they meet torque extrema adjacent to the initial zero crossing. We have not implemented this mechanism on our data set of objects but have carried out initial experiments with an artificial ellipsoid. The results of this experimentation give intuitively sensible results and will appear in a future report.

Some notes should be made about the above framework. Obviously there is an arbitrary choice to be made as to whether we try to span as much of the force dimensions or the torque dimension. This choice will be dependent on the task we wish to accomplish. If the task is merely to pick up the object then the force dimensions are the most important as the torque reference point is the center of gravity, and the gravity vector will have no torque with respect to this point, or very little torque due to small errors in the estimation of the center of mass. If large errors are present then torque becomes more important.

An analysis of 3D wrench space for the planar case (details of which we omit here), has shown that torque extrema either side of a torque zero crossing occur when the distance along the surface normal, measured from the surface to a perpendicular dropped from the center of mass to the normal, is equal to the radius of curvature at that point. Indeed the perpendicular is also a perpendicular to the evolute. In the 3D case the role of the evolute is played by the focal surface and a similar effect occurs.

When splitting a virtual finger into two real fingers in the 2D case, there is only one choice of direction to abduct (spread) the fingers. In the 3D case the choice of direction is unconstrained. We suggest that a sensible choice of direction would be along the direction of minimum principal curvature. Again, initial experiments with an simple shapes suggest that this works well.

A general problem with any wrench space approach is that wrench space consists of dimensions of force and torque which have different units. An arbitrary scaling is therefore introduced to equate force and torque when computing a grasp quality measure. In our work we normalise the torques with respect to the largest torque magnitude which is then given the value one.

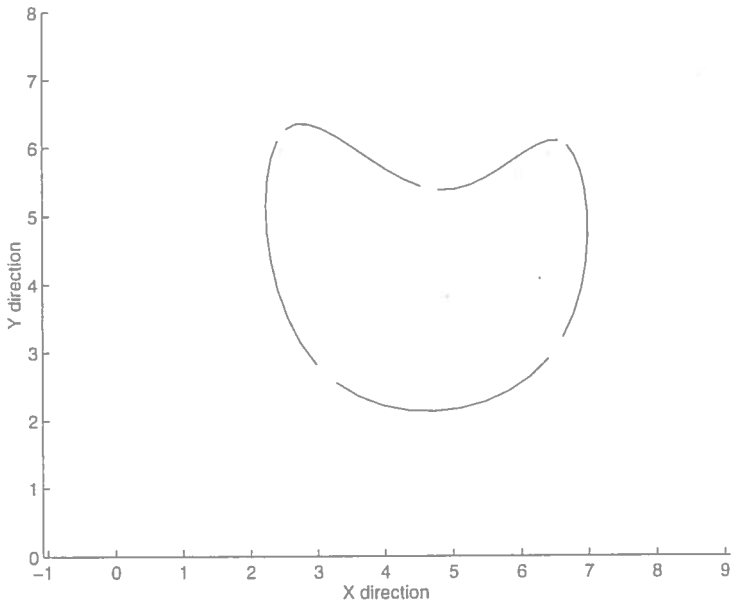

Figure 1: An object boundary modelled using cubic B-splines

6 Our wrench space analysis

In this section we clarify the wrench space analysis by means of a simple example. We illustrate the grasp quality measure used by Pollard and also show how friction is added to the analysis. We do this using a planar object and 3D wrench space although the main work is carried out for 3D objects and a full 6D wrench space. This is because of the impossibility of showing a 6D wrench space.

In Figure 1 we see a simple smooth planar curve. Our goal is to achieve a good grasp of this object. Figure 2 shows the unit object wrench space, which is obtained by applying a unit force to the shape boundary along the inward boundary normal. This curve lies on the surface of a unit cylinder which defines the limit wrench space. To aid visualisation, in Figure 3, we show the curve on the cylindrical surface "unwrapped".

We now apply friction to this picture. Figure 4 shows the *object wrench space including friction* which is obtained by applying a unit force to the shape boundary along the inward boundary normal and additionally within a specified friction cone at each boundary point. The ribbon so formed lies on the surface of a cylinder which defines the limit wrench space. It is a ribbon because a portion of a sine wave is generated side ways from each point on the original single line as the vector swings from one side of the friction cone to the other. In Figure 5 we again show the surface unwrapped to aid visualisation. We can see that the ribbon occupies a large range of the cylinder allowing the possibility of grasps of better quality.

We now choose an initial grasp and evaluate its quality. Figure 6 shows three contact points of an initial grasp. The grasp wrench space of this grasp is shown in Figure 7. This consists of three lines on the wall of the limit wrench space cylinder. Each line is a slice of the "ribbon" of the entire object wrench space including friction. We then compute the convex hull of these lines which is shown in figure 8. The grasp quality measure is the size of the biggest sphere, centered at the wrench space origin, which fits inside this hull. This is shown in Figure 9 and it can be seen that this is small for this grasp, so the grasp is poor.

In an attempt to improve the grasp we add a fourth finger to the object boundary as shown in Figure 10. The grasp wrench space is shown in Figure 11 and an extra line is seen on the right of the cylinder. The convex hull is computed, and this is shown in Figure 12; this can be interpreted

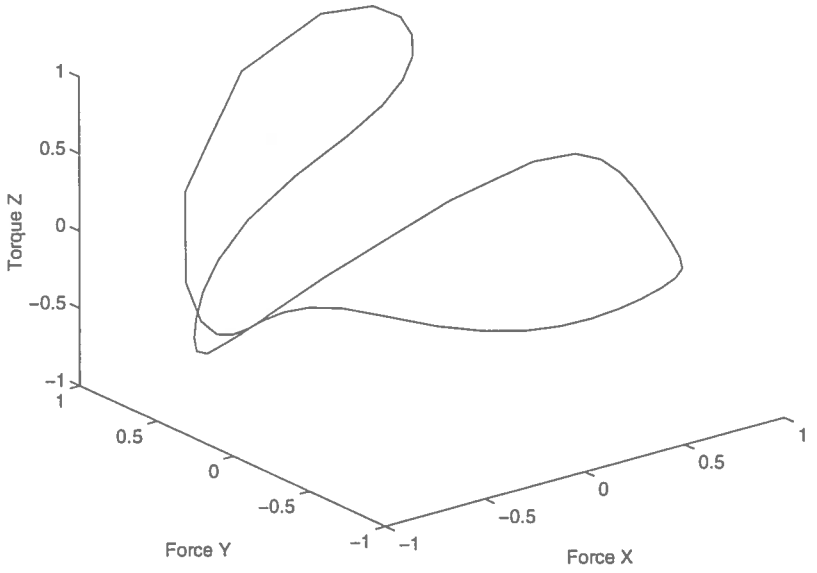

The object wrench space is obtained by applying a unit force to the shape boundary along the inward boundary normal. The curve lies on the surface of a cylinder which defines the limit wrench space.

Figure 2: The object wrench space

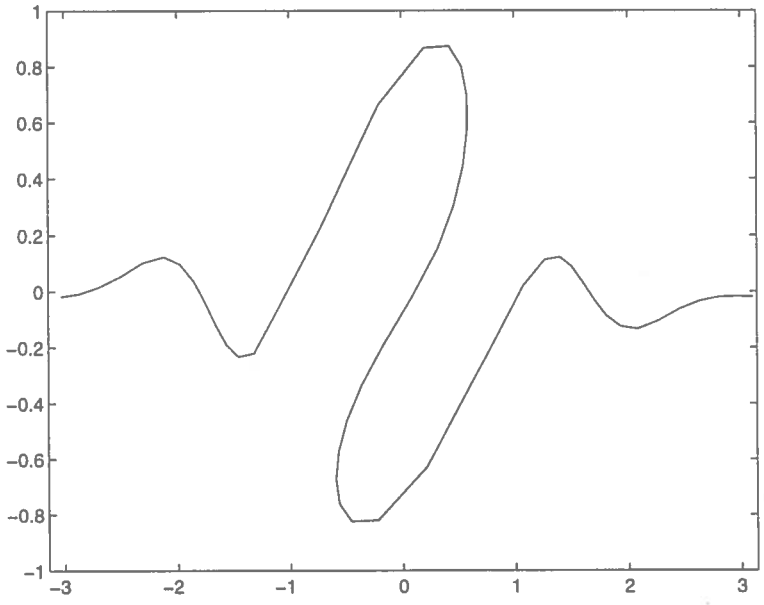

The unwrapped surface of the cylinder on which the the object wrench space curve lies.

Figure 3: The object wrench space unwrapped

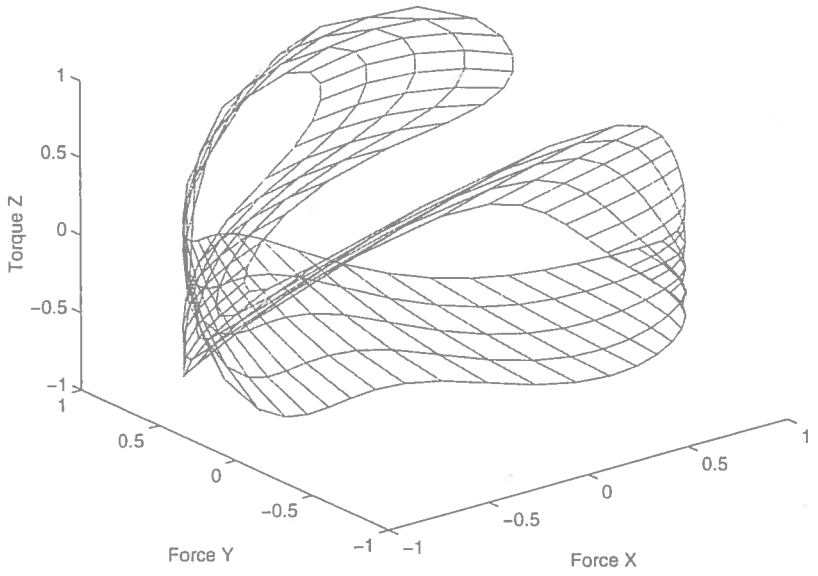

The object wrench space including friction is obtained by applying a unit forces within a specified friction cone at each boundary point. The ribbon so formed lies on the surface of a cylinder which defines the limit wrench space.

Figure 4: The object wrench space including friction

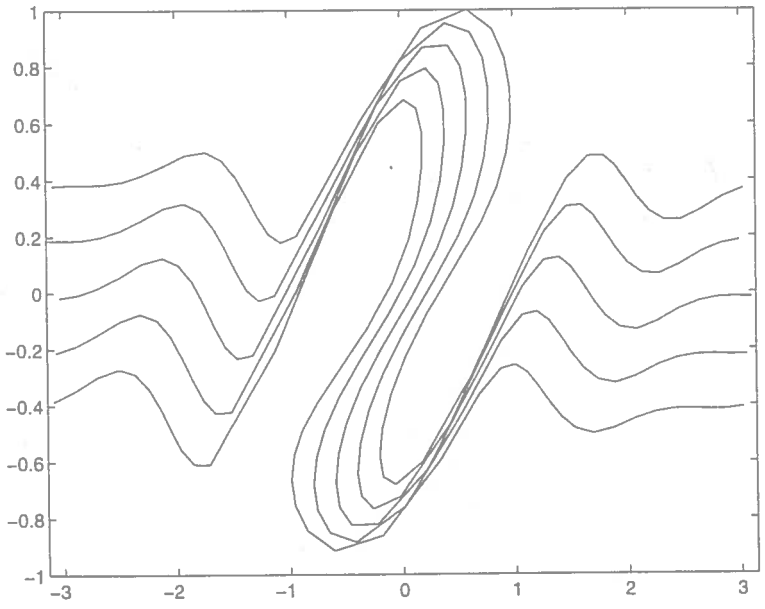

The unwrapped surface of the cylinder on which the ribbon of the object wrench space including friction lies.

Figure 5: The object wrench space including friction unwrapped

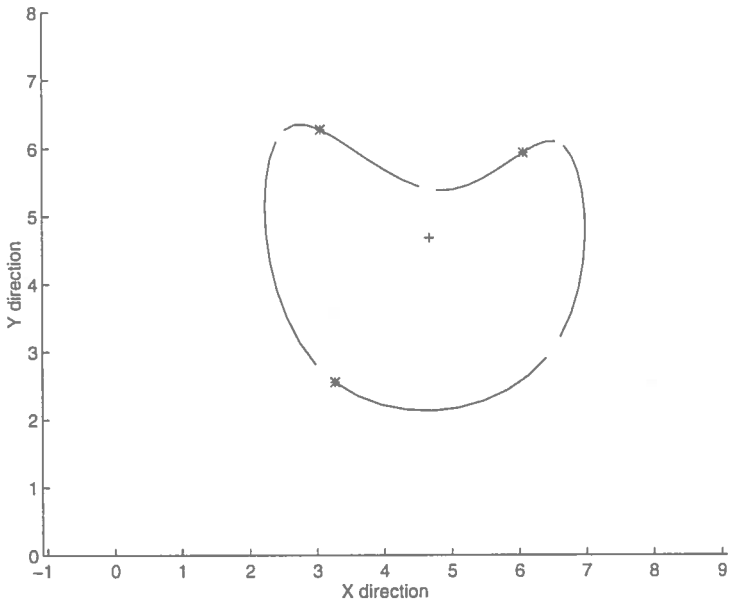

Figure 6: A 2D object with 3 contacts.

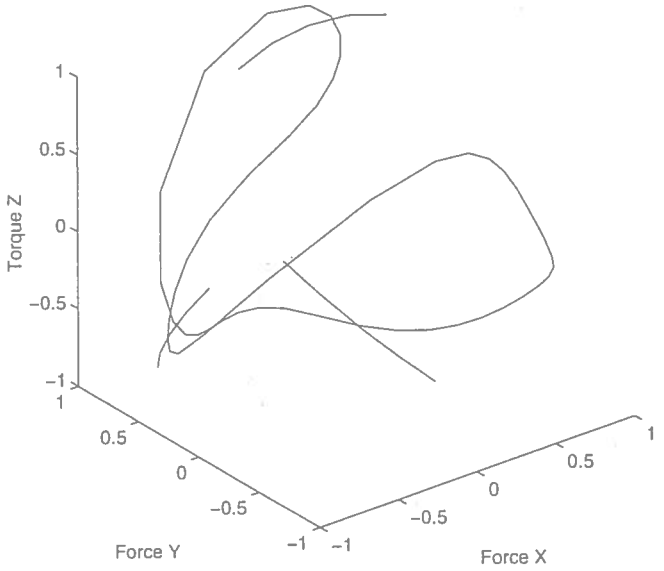

The grasp wrench space including friction for the three point grasp consists of three lines on the wall of a cylinder. Each line is a slice of the "ribbon" of the entire object wrench space including friction.

Figure 7: The grasp wrench space including friction for 3 contacts

as a superset of the original hull,(compare Figure 8). The grasp quality is again computed, the wrench space sphere is shown in Figure 13. It can be seen that the sphere is much bigger (compare Figure 9), confirming that a better grasp has been achieved.

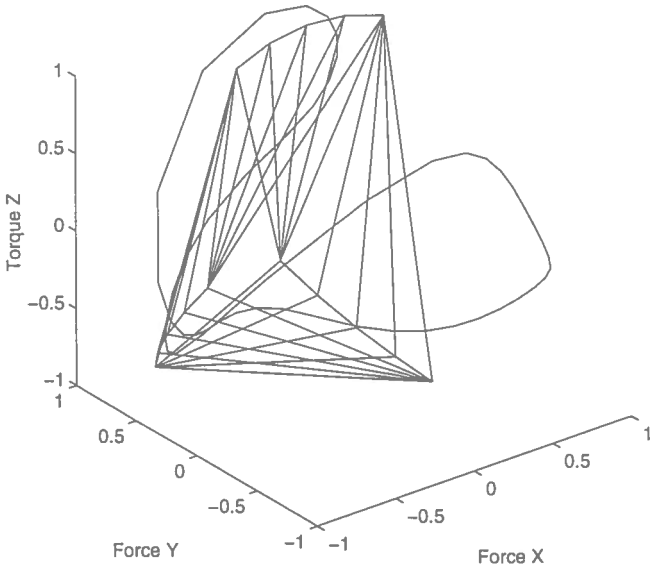

Figure 8: The convex hull of the grasp wrench space including friction for 3 contacts

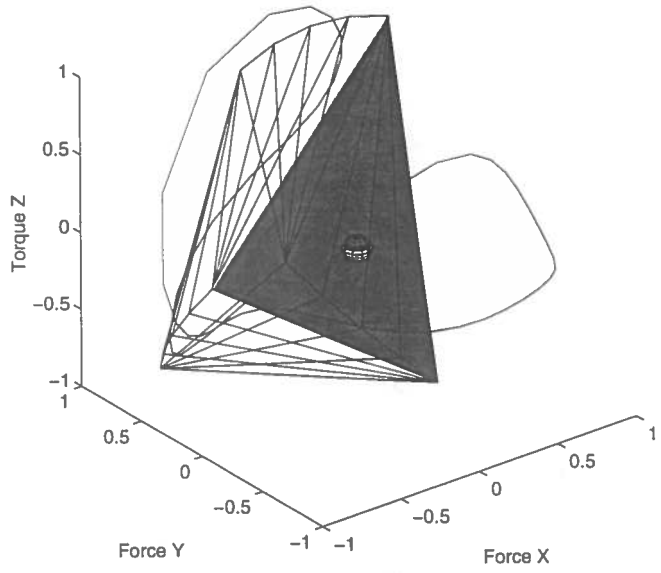

The grasp quality measure is the radius of the largest sphere centered at the origin which can fit inside the convex hull of the grasp wrench space. For the case of these three contact positions the radius is small. The shaded facet is the one nearest that the sphere touches and is therefore nearest to.

Figure 9: The wrench space sphere for the 3 contact grasp

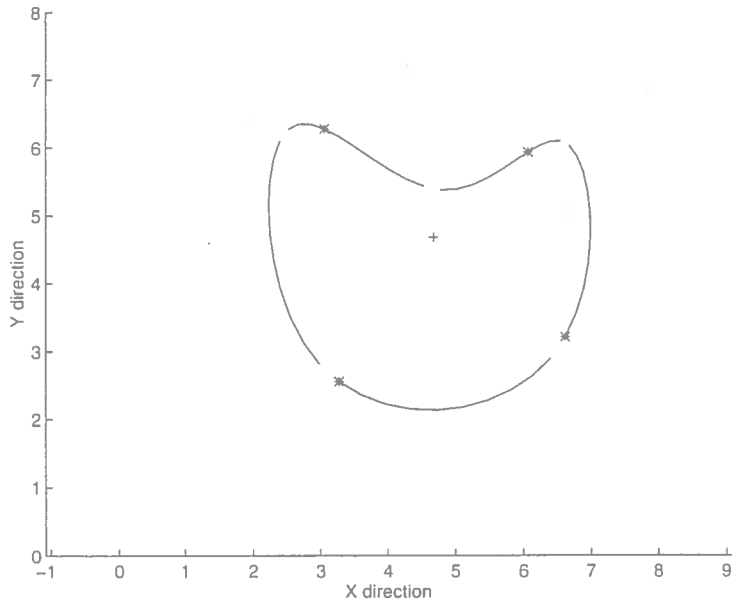

A fourth finger position has been added in an attempt to improve the grasp quality.

Figure 10: An object with 4 contact points

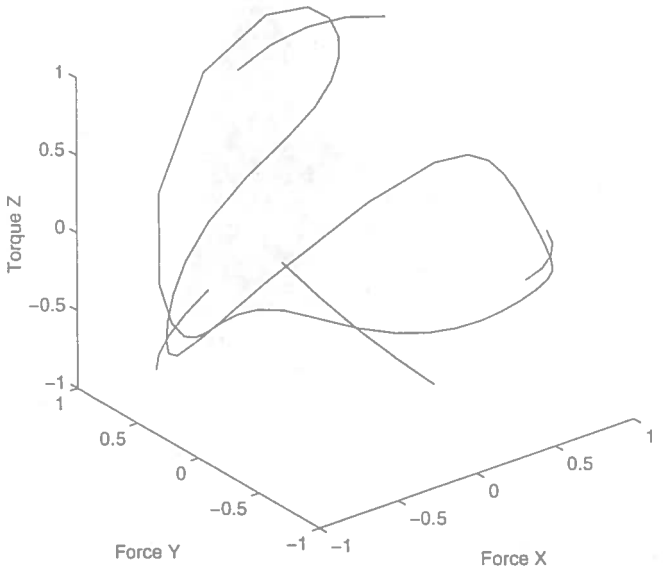

Figure 11: The grasp wrench space including friction with the extra fourth contact.

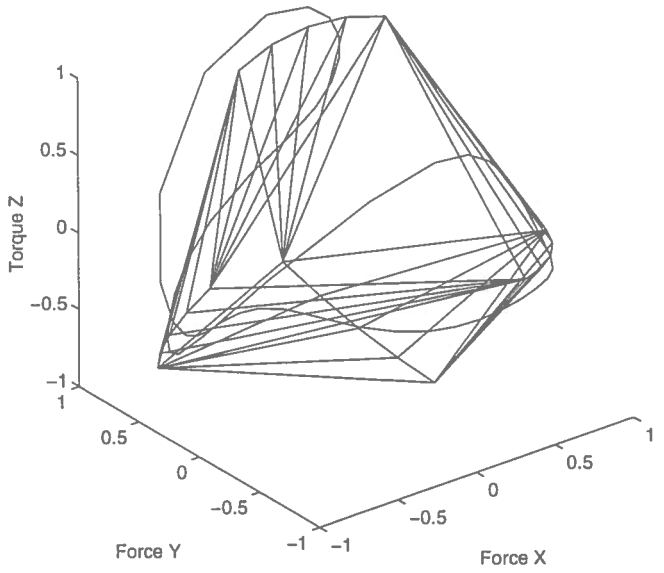

The convex hull of the grasp wrench space including friction is larger than that for three fingers.

Figure 12: The convex hull of the grasp wrench space with friction for 4 contacts

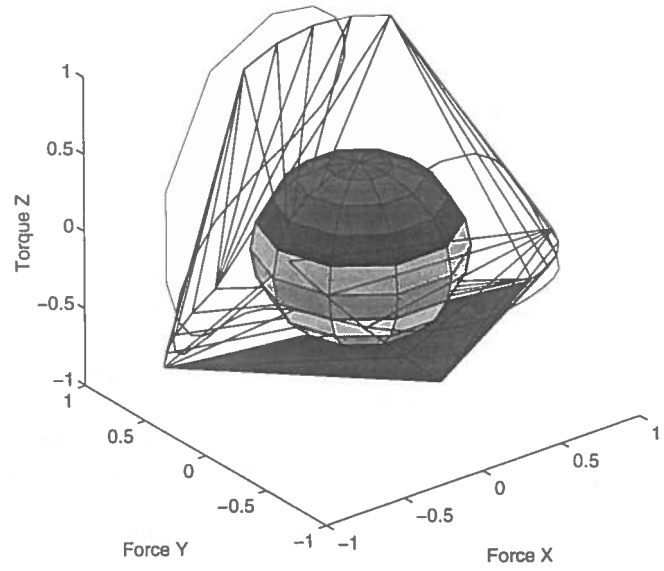

The radius of the wrench space sphere is larger than for the 3 contact grasp. The grasp quality has been improved by applying the fourth contact.

Figure 13: The wrench space sphere for the 4 contact grasp

7 The grasp synthesis

In this section we outline the stages in the synthesis of grasps. The input to the grasp synthesis is meshed surface patch descriptions from the range data segmentation module. The output is a ranking of possible grasps using zero torque contacts, *i.e.* contacts where the surface normal goes through the centre of mass. This has been done for two and three finger combinations. The stages involved in obtaining the grasp rankings are as follows.

1. Torque with respect to the centre of mass is computed for all surface normals to find the biggest torque present for normalisation of the torque in wrench space.

2. Zero crossings of torque are found for each surface patch. This is done by computing the torque for each node on the patch mesh and then simply checking to see if each pixel is a local minimum, *i.e.* that it is lower than its neighbours. If it is then this is put forward as a candidate contact point.

3. All the candidate contact points are collated together. Combinatorical combinations of two and three fingers are computed for this set of candidates. Each combination consists of two or three of the candidate contacts.

4. A typical coefficient of friction is assumed. From this a "canonical" friction cone is generated. The friction cone is approximated by a number of unit vectors around its circumference. In these experiments the cone half angle was $\pi/4$ and the number of approximating vectors was six. An extra unit vector is added at the centre of the cone.

5. The canonical friction cone is transformed so that its central vector points along each of the candidate contact normals in turn. The force and torque components w.r.t the x, y, z axes are computed. This process generates a grasp wrench space including friction for the grasp contact combination.

6. To test for force closure and deduce the grasp quality we need to to generate the convex hull of this grasp wrench space. Once this is done the radius of the wrench space sphere is calculated which is used as the grasp quality measure.

7. Once the above processes have been repeated for all candidate combinations they are sorted in order of their wrench sphere radii with the best grasps having a largest value. This radius is bounded by unity due to the unit force vectors forming a hyper-cylinder.

Some notable points about the grasp synthesis are as follows:

Before the set of grasp wrench points are fed to the convex hull algorithm we add to this set the origin of the wrench space as an extra point. If there is no force closure then the origin will appear on the convex hull and the radius of the wrench space sphere will be zero. If there is force closure, the origin will be inside the convex hull and will not effect the final result.

During our analysis of wrench space we produced a new approximate convex hull algorithm based on the R, θ mapping of the Hough transform. If we map the image curve into R, θ space then the upper envelope of the R, θ curve corresponds to the convex hull in image space. An accompanying report gives further details of this algorithm along with further interesting insights into the properties of the R, θ mapping. A drawback of the algorithm is an exponential increase in memory requirements with increased dimensions, so for the 6D wrench space of the 3D objects we used a proprietary convex hull algorithm called Quick Hull.

8 Experiments

In this section we present the results of running our grasp synthesis algorithm on a data set consisting of range data from several real objects which were previously unmodelled. Results for each object consist of:

- A gray level image of the object.
- A torque encoded mesh plot of the object. This consists of the meshed surface patches of the object which are encoded to show the torque w.r.t to the centre of mass for each point on the surface. Torque zero crossings are denoted by a dark circular patch or dark band on the object surface.
- The candidate contacts (complete with friction cones). These are numbered so that a comparison can be made between different grasps and their grasp qualities to verify that then make intuitive sense.
- Most of the objects have two tables which contain the combination of contacts evaluated for two and three finger grasps and their corresponding grasp qualities. These are sorted with the largest radii and therefore best grasps at the top. If a radius is zero then this means that the grasp was not force closed.

9 Discussion of results

In this section we discuss the results of the last section and make comments about the effectiveness of the approach.

The approach certainly works well for the polyhedral objects. Figure 14 is a picture of a cube. There is a torque zero crossing in the middle of each face of the cube, as can be seen in Figure 15. Figure 16 shows the candidate contacts with their friction cones. The contacts 1 and 4 are the same patch which has been duplicated in the range image registration process. The normals do not meet perfectly at the centre of mass because of subsampling in the algorithm. Little if anything is gained in grasp quality by the extra finger in the three finger case. Parallel facing sides are the best "antipodal" grasps as one would intuitively expect. The prism shows a similar pattern with torque zero crossings one each face in Figure19. Figure 20 shows that the slanting faces produce a force closure grasp but of poor quality. The best grasps are again "antipodal". No gain is made by the third finger.

The faceted stone of Figure 22 is approximately polygonal. Many grasp combinations are produced and we can see examples where the third finger does give an advantage. This is probably because the faces are no longer perpendicular to one another.

For the smooth stone of Figure 26 and particularly the cone of Figure 50 the dark circle of near zero torque is replaced by a dark band. This is because these objects are approximately cylindrical and surface normals pass through the central axis producing near constant torque. This highlights a limitation of the heuristic. For cylinders the torque zero crossings are not isolated points on the surface but a line. For spheres such as the one in Figure 54 the whole surface is a torque zero if the centre of mass is at the centre of the sphere. For the cone, the range segmentation has fitted two cylindrical surfaces which are not perfectly registered with the centre of mass and therefore give isolated zero torque crossings. The position of these zero crossings are arbitrary and unstable. We require a method of detecting spheres and cylinders and to deal with them as an exception.

We have not yet performed detail timings of the grasp synthesis algorithms. The 6D convex hull computation takes on the order of a 10th of a second on a sparc 10 workstation for each candidate grasp. The greatest time at present is spent preprocessing the range data object descriptions which take on the order of one minute on a sparc 10 workstation.

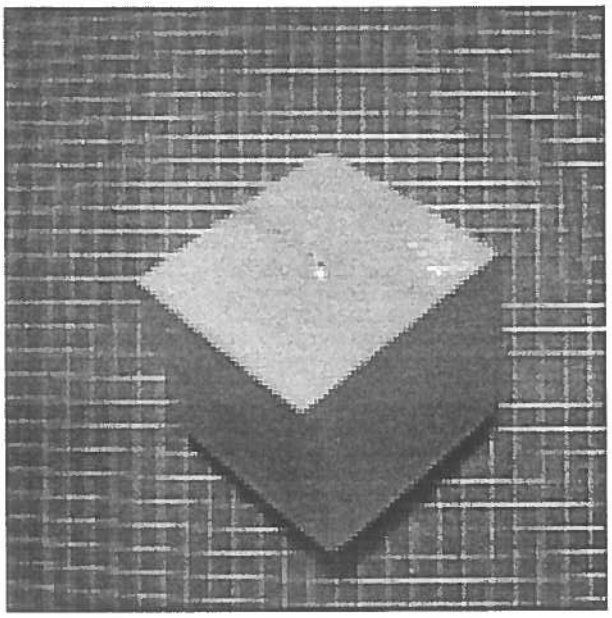

Figure 14: Grey level image of a cube

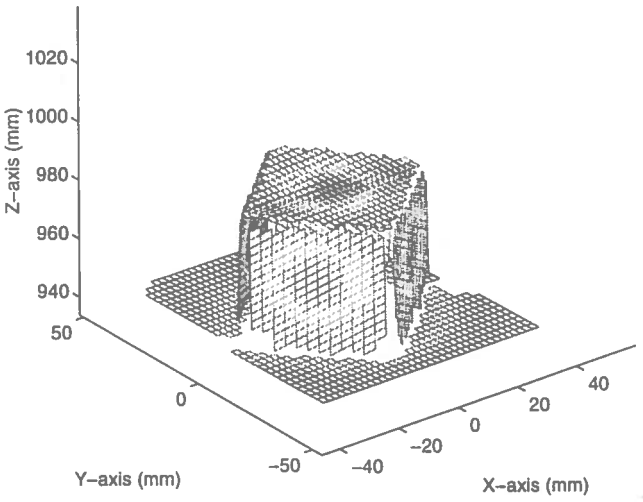

Figure 15: Torque encoded mesh surface of a cube

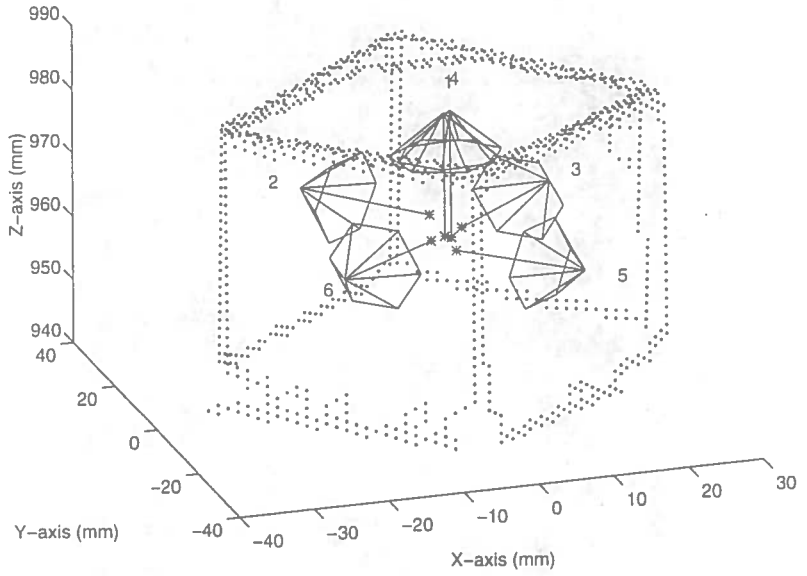

Figure 16: Finger contacts and friction cones at torque minima for a cube

Finger1	*Finger2*	*Radius*
2	5	0.5929
3	6	0.5898
5	6	0.0000
4	6	0.0000
4	5	0.0000
3	5	0.0000
3	4	0.0000
2	6	0.0000
2	4	0.0000
2	3	0.0000
1	6	0.0000
1	5	0.0000
1	4	0.0000
1	3	0.0000
1	2	0.0000

Finger1	*Finger2*	*Finger3*	*Radius*
2	5	6	0.5970
3	5	6	0.5947
2	4	5	0.5929
2	3	5	0.5929
1	2	5	0.5929
2	3	6	0.5909
3	4	6	0.5898
1	3	6	0.5898
1	2	3	0.1536
4	5	6	0.1441
2	4	6	0.1419
3	4	5	0.1364
1	3	5	0.1358
1	2	6	0.1319
1	5	6	0.1224
2	3	4	0.1178
1	4	6	0.0000
1	4	5	0.0000
1	3	4	0.0000
1	2	4	0.0000

Figure 17: Grasp quality in terms of hypersphere radii for two and three finger grasp combinations on a cube

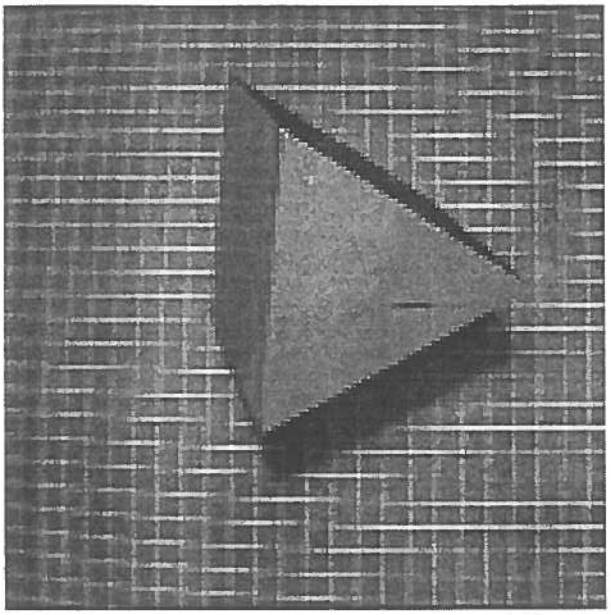

Figure 18: Grey level image of a prism

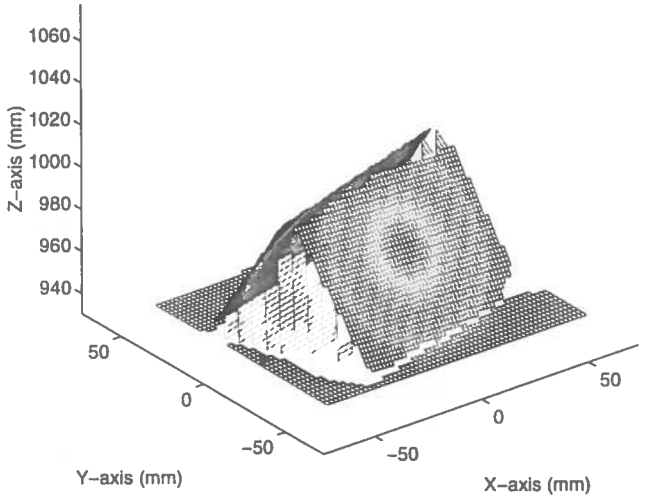

Figure 19: Torque encoded mesh surface of a prism

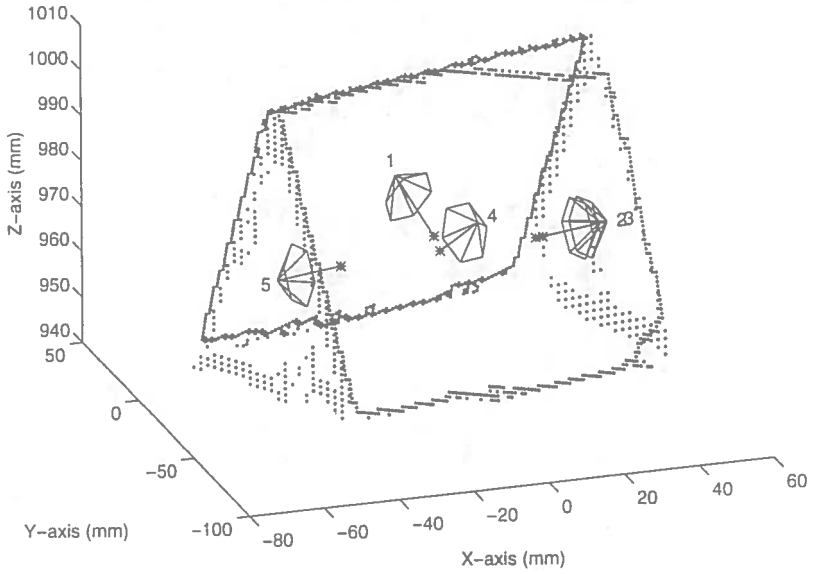

Figure 20: Finger contacts and friction cones at torque minima for a prism

Finger1	*Finger2*	*Radius*
3	5	0.6106
2	5	0.6106
1	4	0.1820
4	5	0.0000
3	4	0.0000
2	4	0.0000
2	3	0.0000
1	5	0.0000
1	3	0.0000
1	2	0.0000

Finger1	*Finger2*	*Finger3*	*Radius*
3	4	5	0.6106
2	4	5	0.6106
2	3	5	0.6106
1	3	5	0.6106
1	2	5	0.6106
1	3	4	0.3020
1	2	4	0.3020
1	4	5	0.3012
2	3	4	0.0000
1	2	3	0.0000

Figure 21: Grasp quality in terms of hypersphere radii for two and three finger grasp combinations on a prism

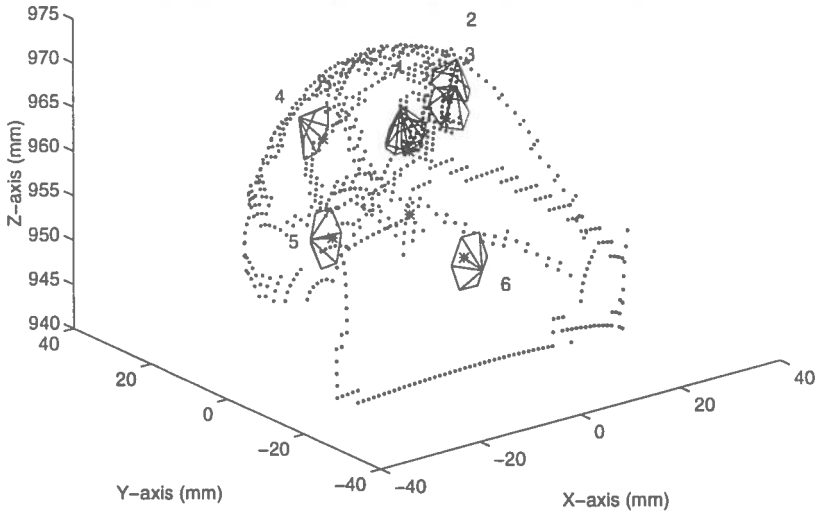

Figure 24: Finger contacts and friction cones at torque minima for a faceted stone

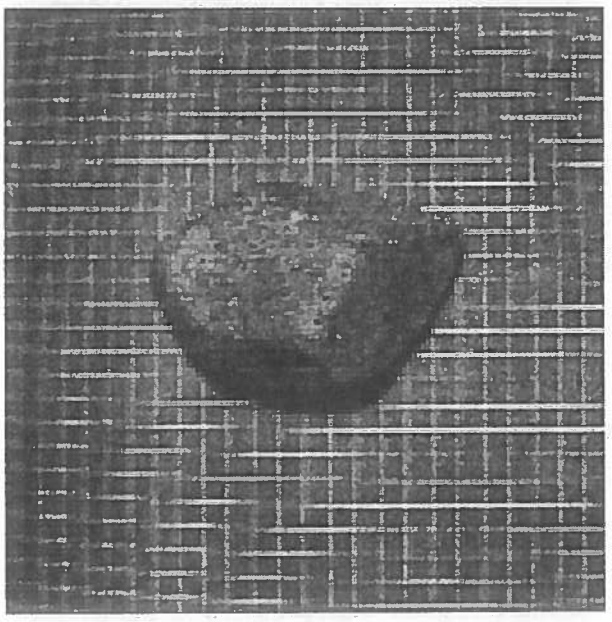

Figure 22: Grey level image of a faceted stone

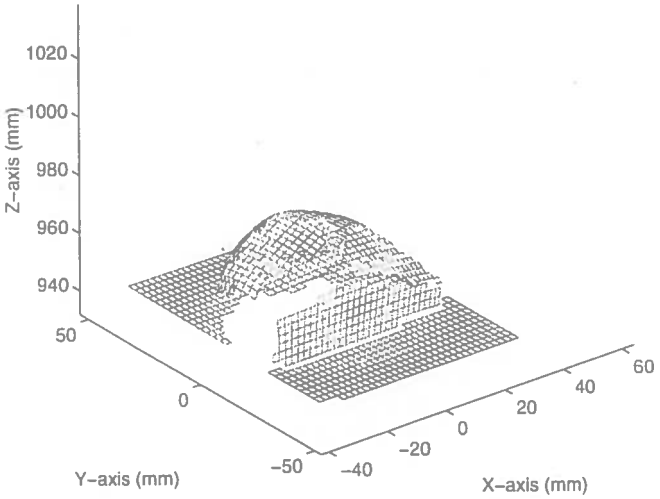

Figure 23: Torque encoded mesh surface of a faceted stone

Finger1	*Finger2*	*Radius*
5	6	0.4996
4	6	0.4592
3	6	0.2148
2	6	0.1519
1	5	0.0773
6	7	0.0323
5	7	0.0105
4	7	0.0000
4	5	0.0000
3	7	0.0000
3	5	0.0000
3	4	0.0000
2	7	0.0000
2	5	0.0000
2	4	0.0000
2	3	0.0000
1	7	0.0000
1	6	0.0000
1	4	0.0000
1	3	0.0000
1	2	0.0000

Finger1	*Finger2*	*Finger3*	*Radius*
3	5	6	0.6156
2	5	6	0.6156
5	6	7	0.6057
1	5	6	0.6006
4	5	6	0.5600
3	4	6	0.5174
2	4	6	0.5174
4	6	7	0.4592
1	4	6	0.4592
3	6	7	0.2722
1	3	6	0.2364
2	3	6	0.2148
2	6	7	0.1740
1	2	6	0.1519
1	5	7	0.0773
1	4	5	0.0773
1	3	5	0.0773
1	2	5	0.0773
2	5	7	0.0544
3	5	7	0.0513
1	6	7	0.0323
4	5	7	0.0105
3	4	7	0.0000
3	4	5	0.0000
2	4	7	0.0000
2	4	5	0.0000
2	3	7	0.0000
2	3	5	0.0000
2	3	4	0.0000
1	4	7	0.0000
1	3	7	0.0000
1	3	4	0.0000
1	2	7	0.0000
1	2	4	0.0000
1	2	3	0.0000

Figure 25: Grasp quality in terms of hypersphere radii for two and three finger grasp combinations on a faceted stone

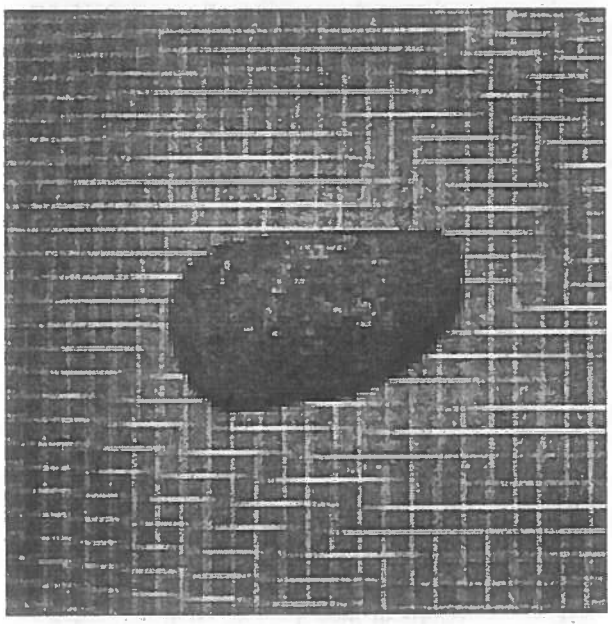

Figure 26: Grey level image of a smooth stone

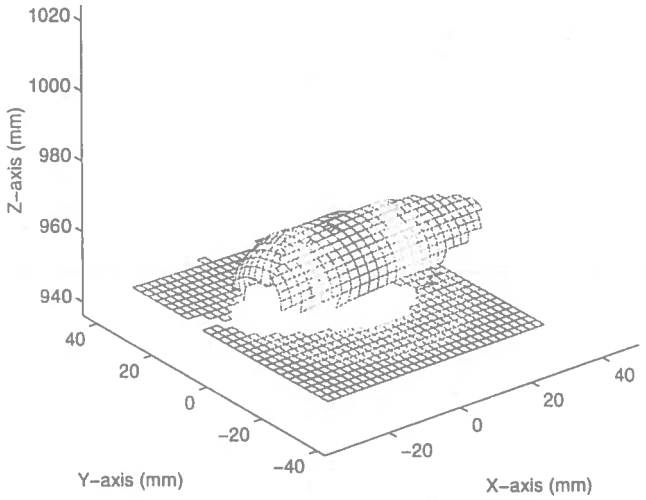

Figure 27: Torque encoded mesh surface of a smooth stone

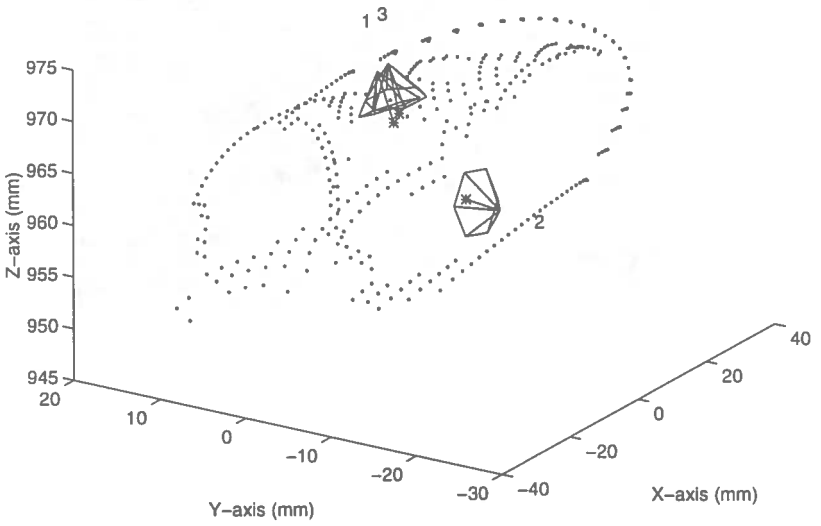

Figure 28: Finger contacts and friction cones at torque minima for a smooth stone

Finger1	*Finger2*	*Radius*
1	2	0.1268
2	3	0.0053
1	3	0.0000

Finger1	*Finger2*	*Finger3*	*Radius*
1	2	3	0.1268

Figure 29: Grasp quality in terms of hypersphere radii for two and three finger grasp combinations on a smooth stone

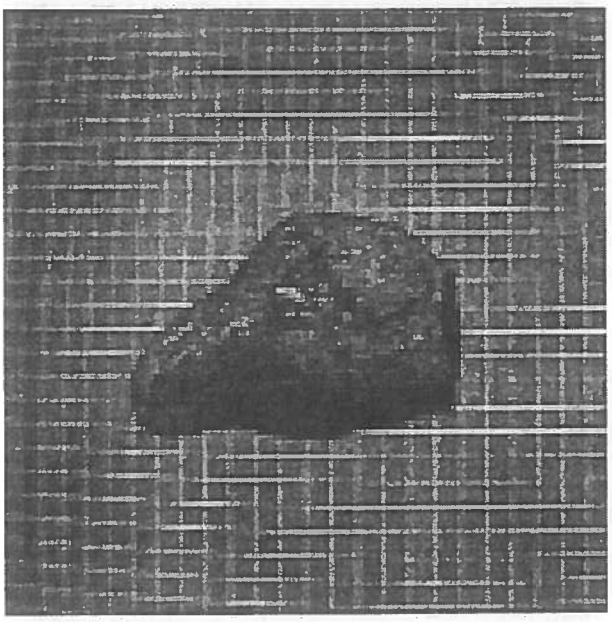

Figure 30: Grey level image of an indented stone

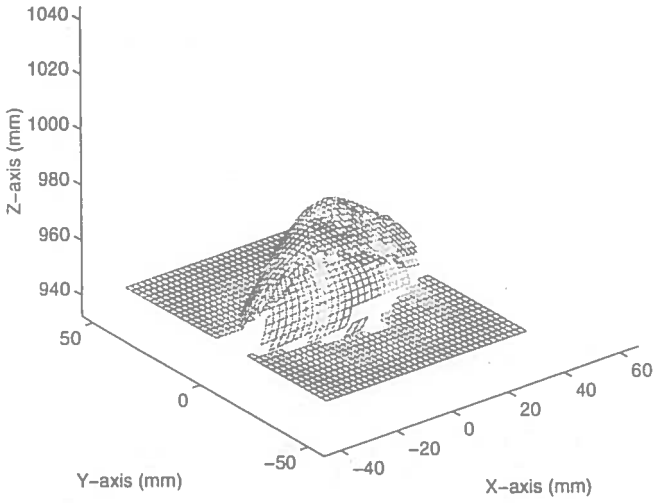

Figure 31: Torque encoded mesh surface of an indented stone

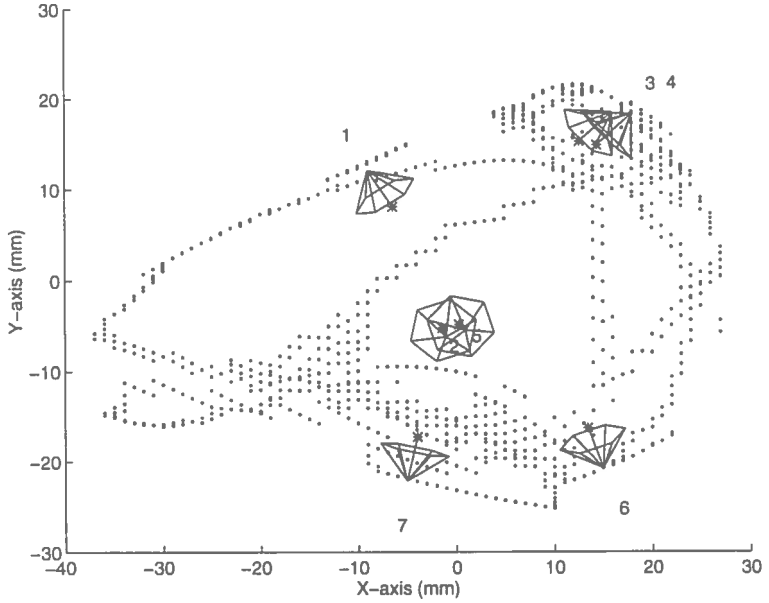

Figure 32: Finger contacts and friction cones at torque minima for a indented stone

Finger1	*Finger2*	*Radius*
1	6	0.5433
4	7	0.4196
3	7	0.3812
1	7	0.3132
3	6	0.2224
4	6	0.1714
5	6	0.0593
6	7	0.0000
5	7	0.0000
4	5	0.0000
3	5	0.0000
3	4	0.0000
2	7	0.0000
2	6	0.0000
2	5	0.0000
2	4	0.0000
2	3	0.0000
1	5	0.0000
1	4	0.0000
1	3	0.0000
1	2	0.0000

Finger1	*Finger2*	*Finger3*	*Radius*
1	3	6	0.6367
1	4	6	0.6239
1	4	7	0.6188
1	5	6	0.5584
1	2	6	0.5584
1	6	7	0.5433
1	3	7	0.5313
4	5	7	0.4234
3	4	7	0.4234
2	4	7	0.4234
4	6	7	0.4196
3	6	7	0.3812
3	5	7	0.3812
2	3	7	0.3812
1	5	7	0.3205
1	2	7	0.3177
4	5	6	0.2720
2	4	6	0.2641
3	5	6	0.2539
2	3	6	0.2508
3	4	6	0.2239
1	2	4	0.0999
5	6	7	0.0593
2	5	6	0.0593
1	4	5	0.0463
1	2	3	0.0257
2	6	7	0.0013
3	4	5	0.0000
2	5	7	0.0000
2	4	5	0.0000
2	3	5	0.0000
2	3	4	0.0000
1	3	5	0.0000
1	3	4	0.0000
1	2	5	0.0000

Figure 33: Grasp quality in terms of hypersphere radii for two and three finger grasp combinations on a indented stone

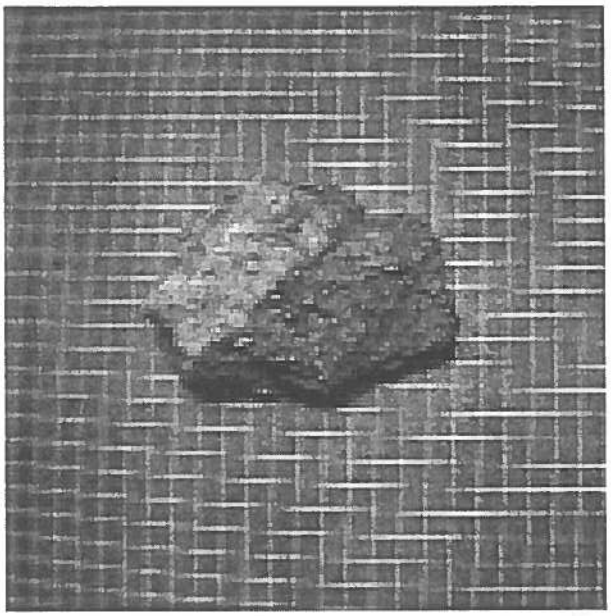

Figure 34: Grey level image of a rough stone

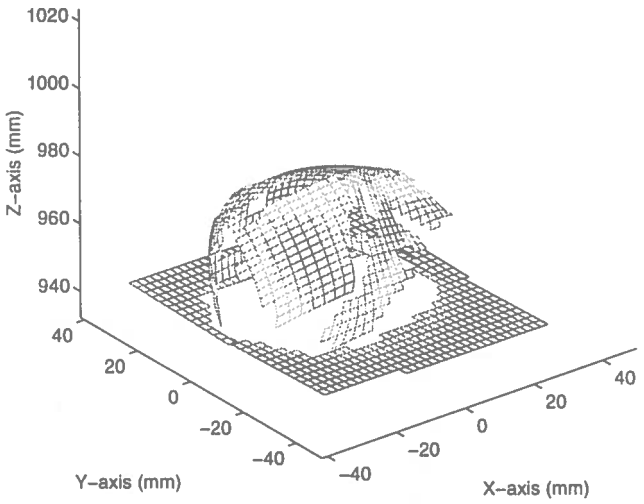

Figure 35: Torque encoded mesh surface of a rough stone

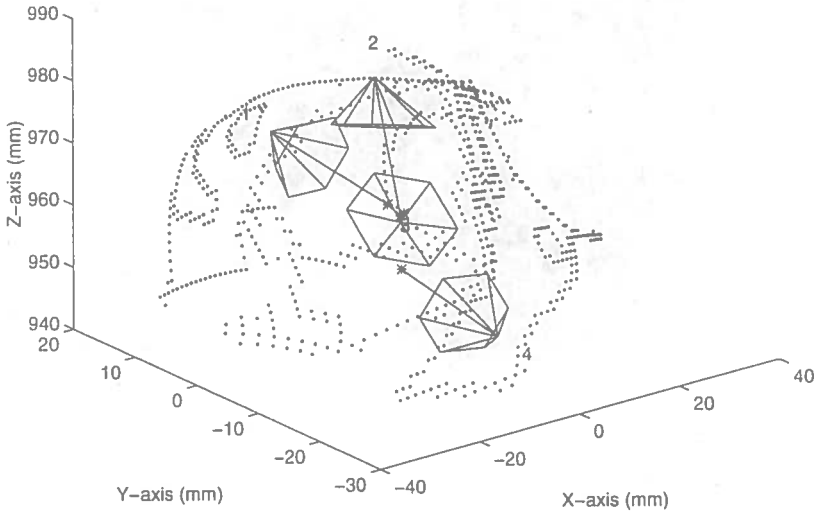

Figure 36: Finger contacts and friction cones at torque minima for a rough stone

Finger1	*Finger2*	*Radius*
1	4	0.5380
1	3	0.2185
2	4	0.2024
2	3	0.0047
3	4	0.0000
1	2	0.0000

Finger1	*Finger2*	*Finger3*	*Radius*
1	3	4	0.5380
1	2	4	0.5380
1	2	3	0.2203
2	3	4	0.2024

Figure 37: Grasp quality in terms of hypersphere radii for two and three finger grasp combinations on a rough stone

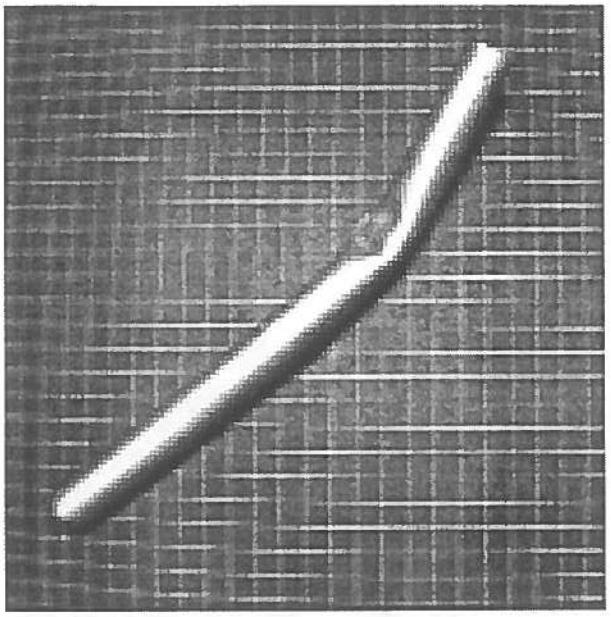

Figure 38: Grey level image of a broken pipe

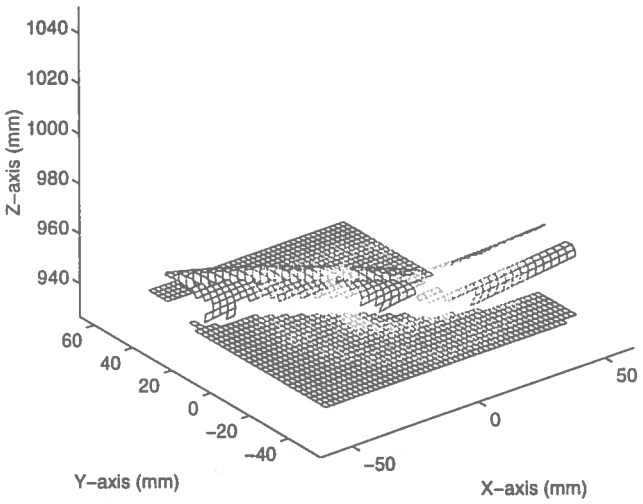

Figure 39: Torque encoded mesh surface of a broken pipe

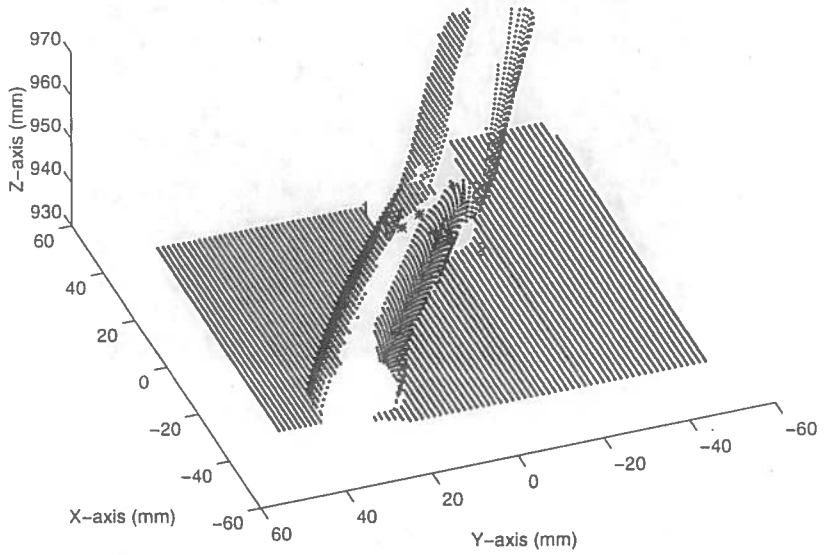

Figure 40: Finger contacts and friction cones at torque minima for a broken pipe

Finger1	*Finger2*	*Radius*
1	2	0.5879

Figure 41: Grasp quality in terms of hypersphere radii for two finger grasp combinations on a broken pipe

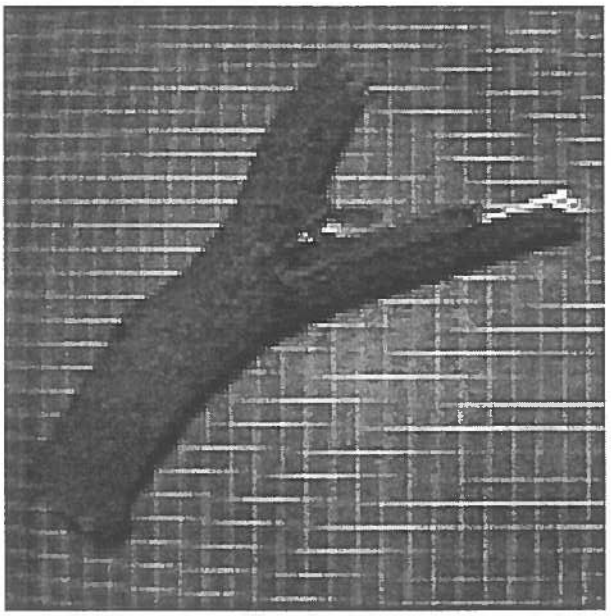

Figure 42: Grey level image of a forked stick

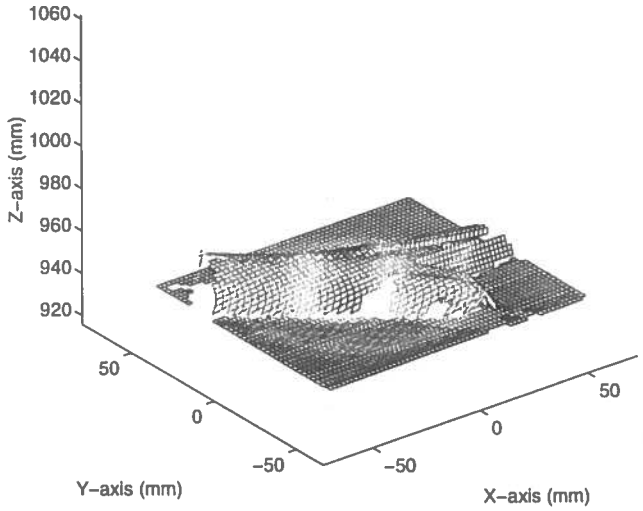

Figure 43: Torque encoded mesh surface of a forked stick

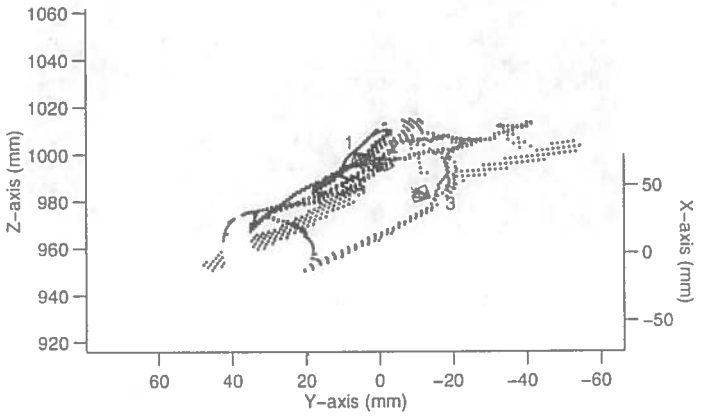

Figure 44: Finger contacts and friction cones at torque minima for a forked stick

Finger1	*Finger2*	*Radius*
1	3	0.3118
2	3	0.0000
1	2	0.0000

Finger1	*Finger2*	*Finger3*	*Radius*
1	2	3	0.3118

Figure 45: Grasp quality in terms of hypersphere radii for two and three finger grasp combinations on a forked stick

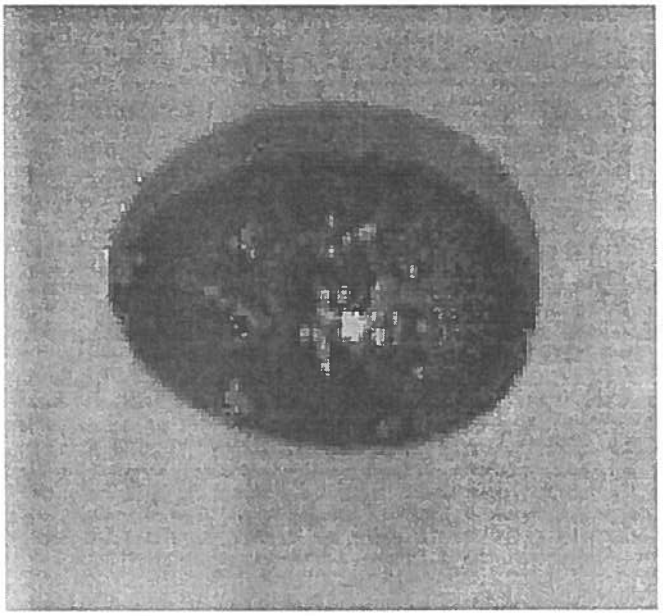

Figure 46: Grey level image of an egg

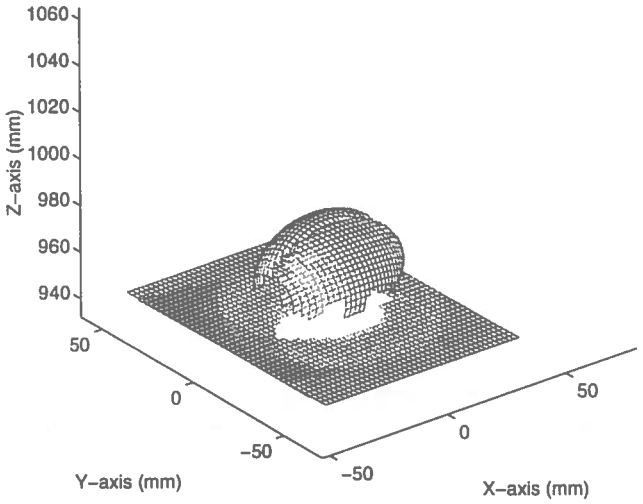

Figure 47: Torque encoded mesh surface of an egg

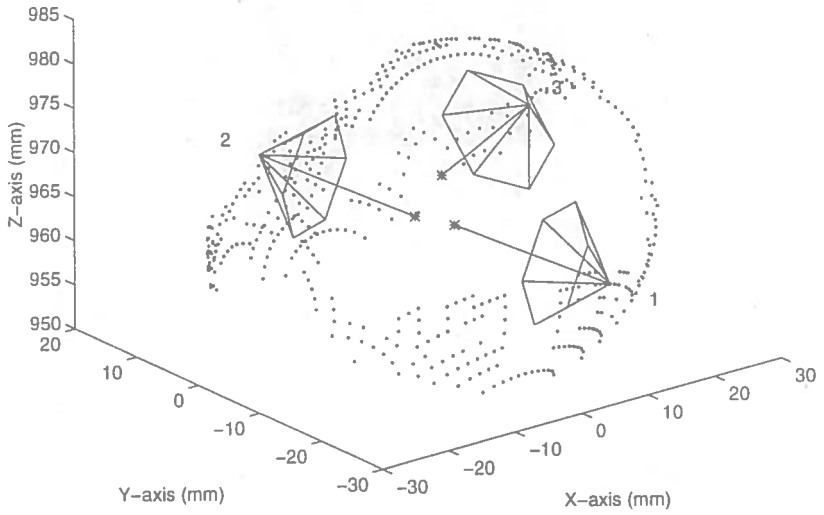

Figure 48: Finger contacts and friction cones at torque minima for an egg

Finger1	*Finger2*	*Radius*
1	2	0.6047
1	3	0.0136
2	3	0.0000

Finger1	*Finger2*	*Finger3*	*Radius*
1	2	3	0.6050

Figure 49: Grasp quality in terms of hypersphere radii for two and three finger grasp combinations on an egg

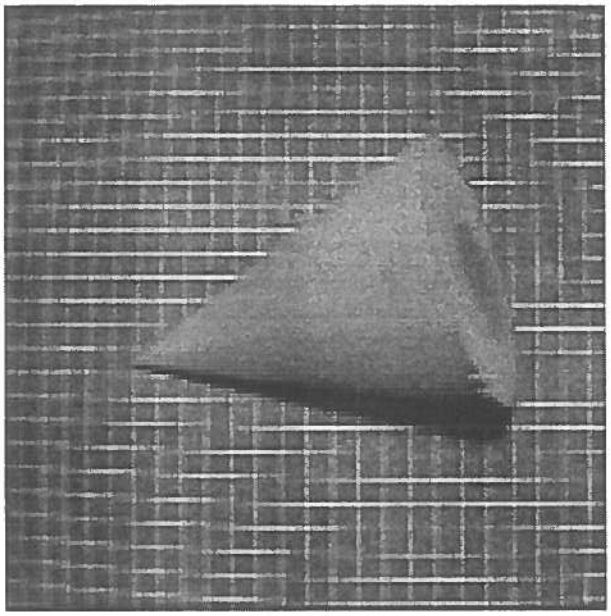

Figure 50: Grey level image of a cone

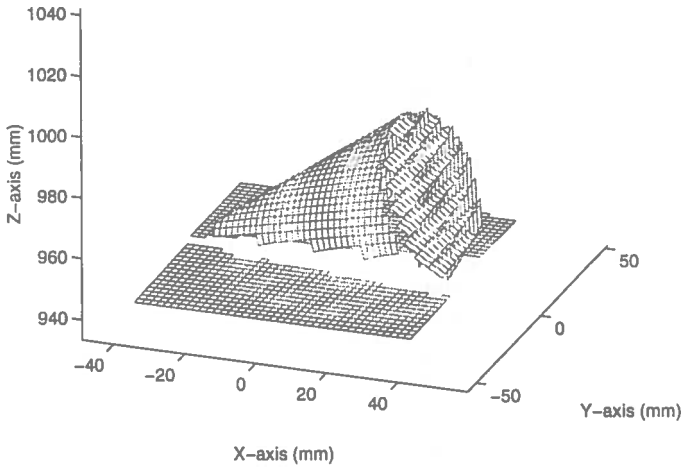

Figure 51: Torque encoded mesh surface of a cone

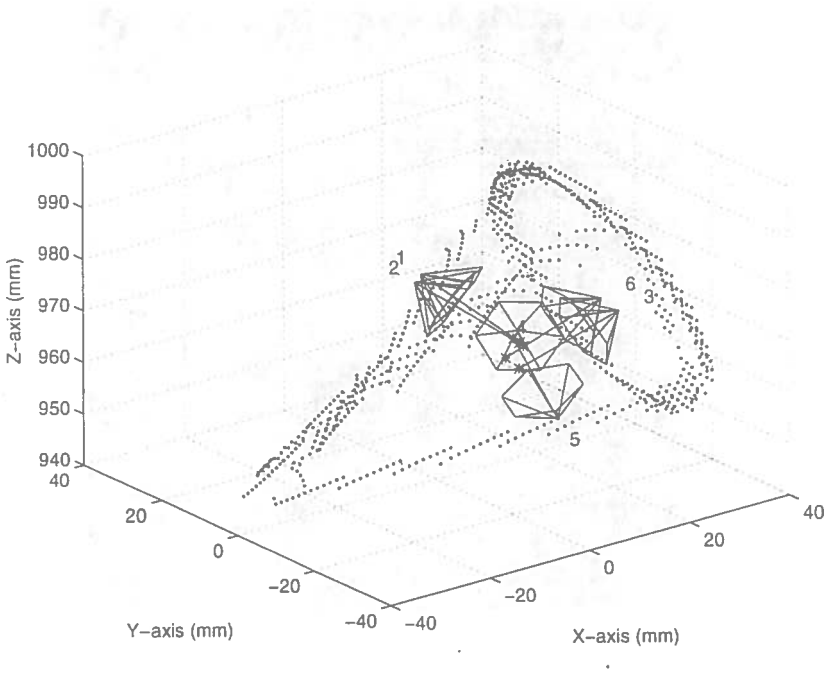

Figure 52: Finger contacts and friction cones at torque minima for a cone

Finger1	*Finger2*	*Radius*
2	5	0.3770
1	5	0.3107
5	6	0.1360
1	3	0.1282
3	5	0.1103
1	6	0.1099
4	6	0.1097
2	3	0.1064
3	4	0.0878
2	6	0.0869
4	5	0.0000
3	6	0.0000
2	4	0.0000
1	4	0.0000
1	2	0.0000

Finger1	*Finger2*	*Finger3*	*Radius*
2	5	6	0.5909
2	3	5	0.5889
1	5	6	0.5322
1	3	5	0.5220
2	4	5	0.3770
1	2	5	0.3770
1	4	5	0.3107
2	3	4	0.2688
2	4	6	0.2683
1	4	6	0.2363
4	5	6	0.2335
1	3	4	0.2310
3	4	5	0.2119
3	5	6	0.1360
1	2	3	0.1282
1	3	6	0.1282
1	2	6	0.1099
3	4	6	0.1097
2	3	6	0.1064
1	2	4	0.0000

Figure 53: Grasp quality in terms of hypersphere radii for two and three finger grasp combinations on a cone

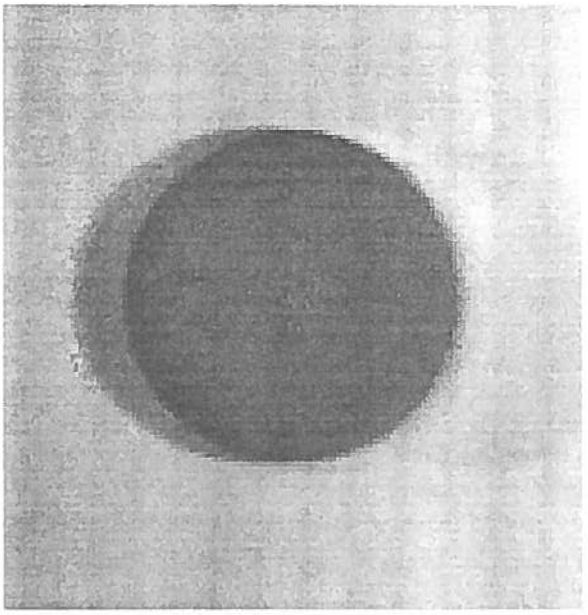

Figure 54: Grey level image of a sphere

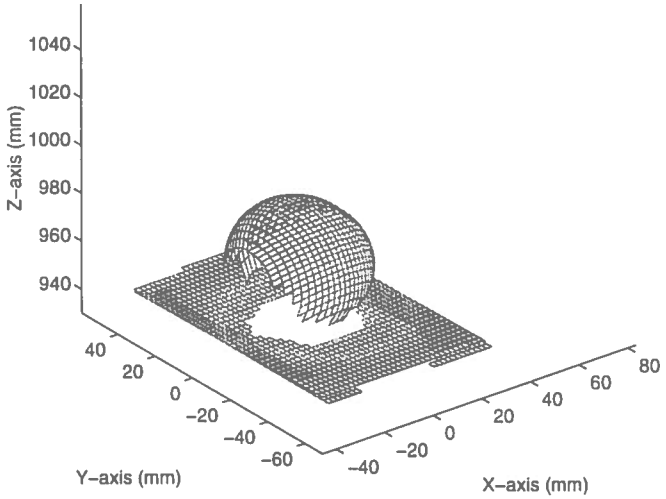

Figure 55: Torque encoded mesh surface of a sphere

10 General comments

If we consider a smooth planar boundary then we can informally define a discriminant surface as formed by the normals to the boundary lifted up to 45 deg from the plane. The number of sheets of the discriminant.over any point of the plane tell us how many normals pass through that point. If we consider the relative position of the centre of mass with respect to the discriminant we can determine the number of torque zero crossings that there will be. (The relationship of the discriminant to the centre of mass also specifies the number and nature of extrema on the object wrench space curve as mentioned in an earlier section). Each type of quadric used in our surface fitting modules will have a qualitatively distinct shape of discriminant and therefore a distinctive signature in terms of how many torque zero crossings it has and their geometric relationship. In the 3D case the discriminant is a 3D surface embedded in a 4D space.

We can consider static and dynamic stability within this framework. If we define a threshold close to zero we can mark patches on the surface which are near to torque zero crossings. The size of the patch is a measure of the zero crossings robustness to modelling error. We can consider the length of the normal measured from the surface to the centre of mass. We suggest that a good heuristic would be to choose contacts where this length is less than the radius of curvature at that point. It is better to hold a rugby ball by diametrically opposite contacts around its central section than contacts placed at its two pointed ends as strong forces applied during manipulation could lead to instability in the latter case.

Despite the offline nature of our grasp synthesis in this feasibility study, we propose that the actual grasp execution should take place within a realtime adaptive force servoing framework.

11 Conclusions

We conclude that grasp synthesis can be successfully driven by range data of unmodelled objects. We have demonstrated this using an extension of Pollard's wrench space analysis. We have added friction to this analysis and made it suitable for precision grasps using multi-fingered hands. We proposed a simple heuristic for finger placement; using contacts where the contact normals go through the centre of mass greatly simplifies the grasp search problem and leads to intuitively consistent results in many cases. A limitation of the heuristic is the case of cylindrical and spherical objects that need to be identified and dealt with separately. It should be noted that much of our work would be valid if another heuristic or theoretical framework were adopted.

12 Further Work

Within the current framework we would implement the finger abduction process proposed in this report. We would also like to feed other grasping frameworks with our data to see how they would cope. For example, it would be a simple matter to search for the anti-podal grasps within Blake's framework. It would be interesting to explore the use of other models such as B-splines. We would like to verify the work using a cheap mobile scanner with less high quality output, and to try to achieve real grasps using a real multi-fingered hand.

Finally, a general multi-fingered theory of grasp remains a future goal for the academic community. From our own work, and reading the work of others, we believe that the path to that goal lies in an understanding of the qualitative structure that shape, symmetry and geometry place on the grasp synthesis problem. Using tools such as differential geometry will allow us to uncover these patterns and use them to synthesise robust grasps efficiently.

References

[1] C. Bard, C. Bellier, C. Laugier, J. Troccaz, G. V ercelli, and B. Triggs. Achieving dextrous grasping by integrating planning and vision based sensing. Technical report, LIFIA-IRIMAG, 1993.

[2] A. Blake. A theory of planar grasp. OUEL Report 1958/92, Oxford University Engineering Department, October 1992.

[3] M.T. Mason and J.K. Salisbury. *Robot Hands and the Mechanics of Manipulation.* MIT Press, 1985.

[4] V.-D. Nguyen. Constructing stable grasps in 3D. In *IEEE International Conference on Robotics and Automation*, volume 1, pages 234–239, 1987.

[5] V.-D. Nguyen. Constructing force-closure grasps. *International Journal of Robotics Research*, 7(3):3–16, 1988.

[6] N.S. Pollard. Parallel methods for synthesizing whole-hand grasps from generalized prototypes. Technical Report AI-TR-1464, MIT Artificial Intelligence Laboratory, 1994.

[7] S.A. Stansfield. Representing generic objects for exploration and recognition. In *IEEE International Conference on Robotics and Automation*, volume 2, pages 1090–1095, 1988.

[8] S.A. Stansfield. Robotic grasping of unknown objects: A knowledge-based approach. *Int. J. of Robotics Research*, 10(4), August 1991.

[9] M.J. Taylor and A. Blake. Grasping the apparent contour. In *Computer Vision - ECCV '94*, volume 1, pages 25–34. Springer-Verlag, 1994.